

# Oxygen measurement in interstitially perfused cellularized constructs cultured in a miniaturized bioreactor

Manuela T. Raimondi<sup>1</sup>, Carmen Giordano<sup>1</sup>, Riccardo Pietrabissa<sup>1,2</sup>

<sup>1</sup>Department of Chemistry, Materials and Chemical Engineering “Giulio Natta”, Politecnico di Milano, Milano - Italy

<sup>2</sup>Department of Information Engineering, University of Brescia “Health and Wealth”, Brescia - Italy

## ABSTRACT

**Aims:** The possibility of developing engineered tissue in vitro and maintaining the cell viability and functionality is primarily related to the possibility of controlling key culture parameters such as oxygen concentration and cell-specific oxygen consumption. We measured these parameters in a three-dimensional (3D) cellularized construct maintained under interstitially perfused culture in a miniaturized bioreactor.

**Methods:** MG63 osteosarcoma cells were seeded at high density on a 3D polystyrene scaffold. The 3D scaffolds were sensorized with sensor foils made of a polymer, which fluoresce with intensity proportional to the local oxygen tension. Images of the sensor foil in contact with the cellularized construct were acquired with a video camera every four hours for six culture days and were elaborated with analytical imaging software to obtain oxygen concentration maps.

**Results:** The data collected indicate a globally decreasing oxygen concentration profile, with a total drop of 28% after six days of culture and an average drop of 10.5% between the inlet and outlet of the perfused construct. Moreover, by importing the measured oxygen concentration data and the cell counts in a model of mass transport, we calculated the cell-specific oxygen consumption over the whole culture period. The consumption increased with oxygen availability and ranged from 0.1 to 0.7  $\mu\text{mol}/\text{h}/10^6$  cells.

**Conclusions:** The sensors used here allowed a non-invasive, contamination-free and non-destructive oxygen measurement over the whole culture period. This study is the basis for optimization of the culture parameters involved in oxygen supply, in order to guarantee maintenance of cell viability in our system.

**Keywords:** Microfluidics, Cell culture, Perfusion, Bioreactor, Oxygen, Sensor

## Introduction

The goal of creating engineered biological tissues can be achieved by using culture devices known as bioreactors. A bioreactor is defined as a device for the in vitro development of living, functional tissues, but can be also seen as a dynamic culture model system to study fundamental mechanisms of cell function under physiologically relevant conditions (1). In fact, cells in a biological environment are subjected to multiple regulatory signals (e.g. growth factors, hydrodynamic, electrochemical and mechanical stimuli), which are simulated in the artificial and experimental setting. Studies have discov-

ered that three-dimensional (3D) scaffolds offer the possibility of culturing higher cell densities, support visualization, and resemble the biological environments more efficiently than the two-dimensional (2D) monolayer (2). In bioreactors, 3D scaffolds are positioned inside a culture chamber and are perfused with a culture medium which ensures the convective transport of solutes ( $\text{O}_2$ , metabolites, catabolites, etc.) to and from the superficial regions of the construct.

The success of bioreactor culture widely depends on oxygen gradient within the scaffold as oxygen plays an important role in various cell functions. Oxygen is required for the aerobic metabolism of carbon compounds and consequently impacts cell growth rate and protein synthesis; furthermore, it enhances the correct differentiation of stem cells. In constructs perfused only superficially, the resulting oxygen distribution is not homogeneous throughout the 3D construct volume because of the lack of interstitial flow and due to the low solubility of oxygen in the culture medium (3), which may lead to hypoxia. The presence of a better quantified local oxygenation is a condition required to avoid areas of hypoxia and to better control cell response in the cultured cellular constructs.

Different methods have been employed in order to quantify oxygen consumption and concentration drop in 3D

Accepted: June 8, 2015

Published online: October 7, 2015

### Corresponding author:

Manuela T. Raimondi  
Department of Chemistry  
Materials and Chemical Engineering  
“Giulio Natta” Politecnico di Milano  
32, piazza L. da Vinci  
20133 Milano, Italy  
manuela.raimondi@polimi.it

bioreactor-cultured constructs. For example, Cioffi implemented a combined experimental/computational approach to quantify oxygen transport to human chondrocytes cultured in 3D scaffolds in a perfusion bioreactor system (4). This study collected data which refer to a global difference of oxygen concentration between the inlet and outlet regions of the bioreactor, without focusing on the inner and local oxygen distribution within the cellularized construct. Evaluation of the local oxygen profiles within 3D constructs introduces further difficulties. Wang exploited optical, luminescence-based oxygen sensors integrated with a microfluidic cell culture system (5, 6). This group utilized fluorescent micro-particles (so-called beads) distributed within the construct, to sense the local oxygen partial pressures ( $pO_2$ ) in the cell microenvironment, with a maximum calibration error of approximately 25% for  $pO_2$  in the range of 0 to 10 mm Hg. This technique allows ratiometric measurements of temporal changes in oxygen concentrations in transparent 3D scaffolds, by monitoring fluorescence intensity with a fluorescence microscope. The beads calibration and fabrication method had been previously described by Acosta who also demonstrated their non-cytotoxicity and non-oxygen-consuming capability (7). The dimension of oxygen-sensing beads is in the range 5–40  $\mu\text{m}$ . They are built of polydimethylsiloxane (PDMS) and encapsulated in silica gel shell bound with two fluorophores: 1)  $\text{Ru}(\text{Ph}_2\text{phen}_3)\text{Cl}_2$ , an oxygen-sensitive luminophore, and 2) Nile blue chloride, an oxygen-insensitive reference fluorophore. Moreover, these probes have shown good reversibility of oxygen binding, no evidence of hysteresis in their sensing activity, and a great capability of measuring  $pO_2$  in ranges relevant to 3D tissue culture studies. A limitation of oxygen-sensing particles is the presence of a certain heterogeneity in fluorescent dye distribution among the sensing beads. In fact, some of them do not have a fluorescent dye loaded silica core, while others only have Ruth dye signal without corresponding reference dye signal. Although beads that do not fluoresce are excluded during data processing to correct the potential error, this may lead to misinterpretations in areas of interest. Differently, Kellner adopted  $pO_2$  optical sensor foils composed of  $O_2$ -sensitive indicator dyes, which permit to monitor and analyze gradients and oxygen supply in a tissue over a culture period (8). This study evaluates 2D  $pO_2$  distributions across the tissue section in contact with the foil surface. Results refer to cell cultures in spinner flask bioreactors, wherein not all the cells are exposed to the same shear stress and the presence of convective forces does not ensure a uniform nutrients provision.

The target of this work is the measurement of oxygen concentration within a 3D cellularized construct under perfused culture, by the use of a thin-film oxygen sensing system. The cell culture experiments have been conducted using osteosarcoma immortalized cells seeded on polystyrene micro-scaffolds and cultured under interstitial perfusion in a miniaturized bioreactor. The bioreactor chamber was sensorized with an oxygen thin-film sensor, which offers a non-invasive and contamination-free procedure. The transparency of the scaffold biomaterial allowed the use of optical methods to quantitatively map the spatial-temporal fluctuations of oxygen concentration within the tissue-engineered construct in a non-destructive way.

## Materials and methods

### Cell culture and seeding procedure

All reagents used were from EuroClone unless specified differently. Cells were expanded from an immortalized cell line from human osteosarcoma (MG63, Sigma) in a culture medium composed by Minimum Essential Medium (MEM) supplemented with 10% v/v Fetal Bovine Serum (FBS), 1% v/v Non-Essential Amino Acids 100  $\times$  solution (NEAA), 1% v/v Penicillin/Streptomycin 100  $\times$  solution, 1% v/v L-Glutamine 200 mM solution. The goal of obtaining a homogeneous cell distribution within the scaffolds was achieved thanks to a specific dynamic seeding protocol, previously defined by Laganà (9), and briefly reported as follows. Under sterile conditions, each scaffold was placed in a well of a 24 multiwell plate (Corning) and covered with a solution of  $10^6$  cells in 400  $\mu\text{l}$  of medium. The plate was then shaken, under 5%  $\text{CO}_2$  at 37°C in an incubator, by the use of a 3D multifunction rotator (PS-M3D, WWR) for five hours. The 3D rotator was stopped after 5 hours and the seeded scaffolds stayed still overnight before being transferred in clean wells filled with 400  $\mu\text{l}$  of medium. Thereafter the seeded cells were marked, by incubation with 4',6-Diamidino-2-phenylindole dihydrochloride (DAPI, Sigma) at a concentration of 10  $\mu\text{g}/\text{mL}$  in Phosphate Buffer Saline (PBS) for 90 minutes under 5%  $\text{CO}_2$  and 37°C conditions, followed by a twice rinsing with PBS. The seeded scaffolds were then put inside the steam-sterilized bioreactor pre-filled with the culture medium.

### Culture experiments and oxygen estimation

The oxygen sensor foils used for oxygen imaging are the SF-RPSu4 (PreSens, Germany). The sensor foils were cut into rectangular pieces with dimensions of 6 mm  $\times$  3 mm fitting the single culture chamber (Figs. 1A and 1B). They were washed with distilled water, kept in used 70% EtOH for one hour, dried, washed twice in cell culture-grade distilled water and kept wet in complete culture medium until use. The miniaturized bioreactor used in this work has been developed and validated for cell culture in a previous work (9).

Three identical experiments were performed. In each experiment, images of the oxygen sensors were taken every 4 hours uninterruptedly for 6 culture days. At each time step, each acquired image (Fig. 1C) was converted into a map of local oxygen concentration by the use of calibration parameters defining the 0% and 20% oxygen tension. These calibration values were determined during a complete culture experiment performed prior to this study, in conditions identical to those used in this study. The 0% oxygen calibration value was determined by filling with 100% nitrogen the culture chamber and acquiring oxygen maps. The 20% oxygen calibration value (corresponding to saturation) was determined by filling the incubator with fresh atmospheric air and acquiring oxygen maps. Once converted into local oxygen concentration values, the areas corresponding to the whole scaffold surface were subdivided into 12 regions of interest and the mean oxygen concentration was calculated for each region using the PreSens software (Fig. 1D). The average oxygen concentration was finally obtained for each chamber

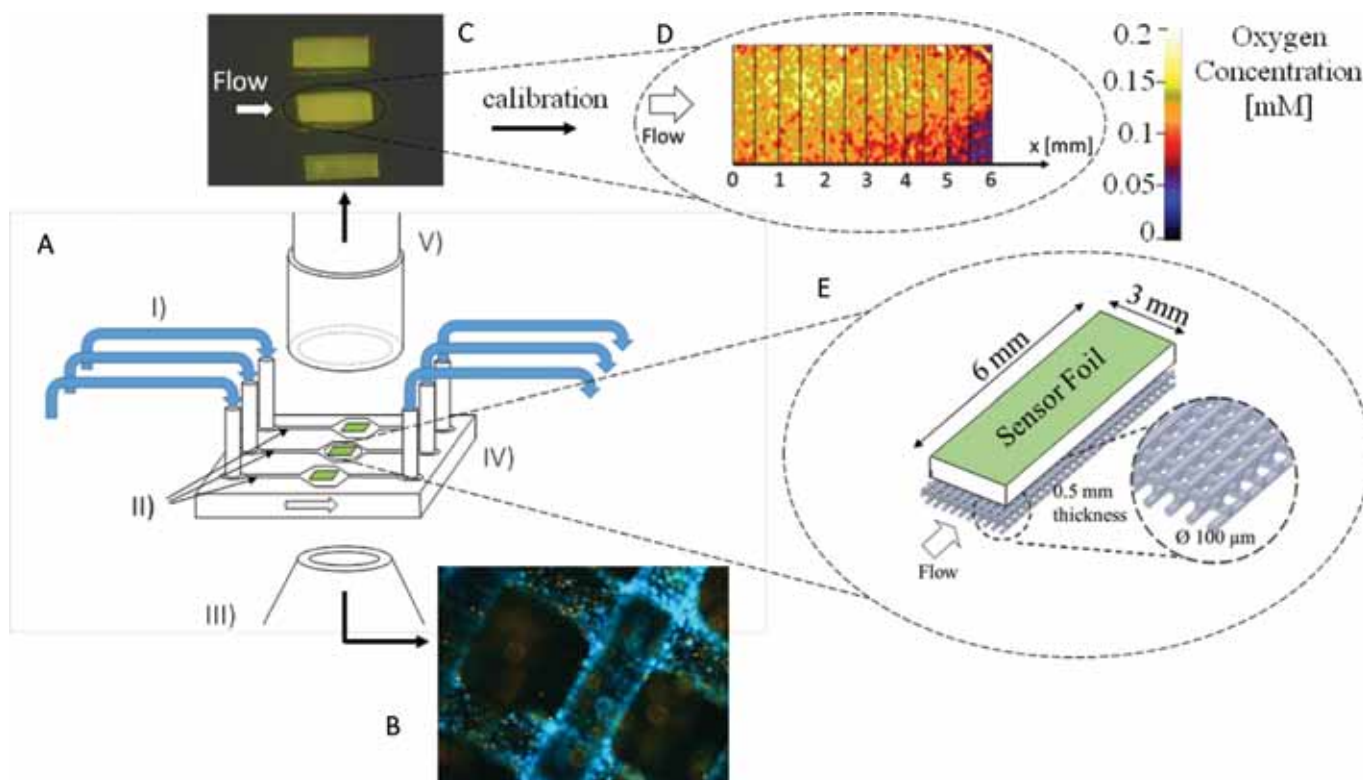


**Fig. 1** - (A) Scheme of the experimental set-up. (I) Cell culture medium is conveyed in the culture chambers by a syringe pump whose flow rate was set to  $7.2 \times 10^{-3}$  mL/min. (II) Microfluidic channels convey the flow in the three independent culture chambers. (III) High resolution fluorescence microscope objective. (IV) Optically accessible miniaturized bioreactor whose chambers contain each a cellularized construct. (V) Oxygen-sensing camera. (B) Video frame, showing the cells adhered onto the scaffold fibers, acquired by fluorescence microscopy and used to estimate cell proliferation. (C) Image of the three sensorized culture chambers acquired by the camera unit. (D) Local oxygen map calibrated with VisiSens AnalytiCal 1 and divided into 12 regions of interest. (E) Micro-structured scaffold fabricated by rapid prototyping, with the oxygen sensor foil placed on its surface. Each cell-seeded-sensorized scaffold is located in an independent culture chamber.

and at each culture time, by averaging the values obtained for the 12 regions of interest. The mean and standard deviation of these averaged concentrations were calculated for the three experiments.

To predict the oxygen consumption rate of the cells in time, we applied a compartmental model of chemical consumption:

$$v = Q(C_1 - C_2) \quad [1]$$

where  $Q$  represents the experimental flow rate which is  $7.2 \times 10^{-3}$  mL/min,  $C_1$  and  $C_2$  are the oxygen concentration of the inlet and outlet regions of the scaffold surface respectively. The oxygen consumption specific to cells was then calculated as follows:

$$V = \frac{v}{N} \quad [2]$$

where  $N$  is the cell density in each scaffold and  $v$  is the cells oxygen consumption calculated through equation (1) measured in  $\mu\text{mol}/\text{min}$ . The cell density in the constructs was measured on live images taken in fluorescence on the DAPI channel (Fig. 1B), every 24 hours at selected time points during each experiment. The mean estimated cell density data

were then interpolated with a cubic spline function to obtain an estimate of the mean scaffold cell density over time.

### Statistical analysis

A two-sample Student's t-test was used to assess the statistical significance of the results for the three experiments, with a cut-off of  $p < 0.05$ . The two groups of samples compared are the mean oxygen concentrations in each region of the scaffolds, at maximum and minimum concentration time, respectively.

### Results

The measurement results are shown in Figure 2 at the various construct regions and in Figure 3 at the various culture times. The oxygen concentration curves are averaged on the three culture chambers. In Figure 2, the two oxygen concentrations reported refer to the culture times in which the maximum and minimum average values were recorded, i.e. the initial time (day 0) and after 1.5 days of culture, respectively. Both oxygen maps in the figure show a higher oxygen concentration in the inlet regions, which decrease towards the outlet. Furthermore, the boundary areas of the scaffold

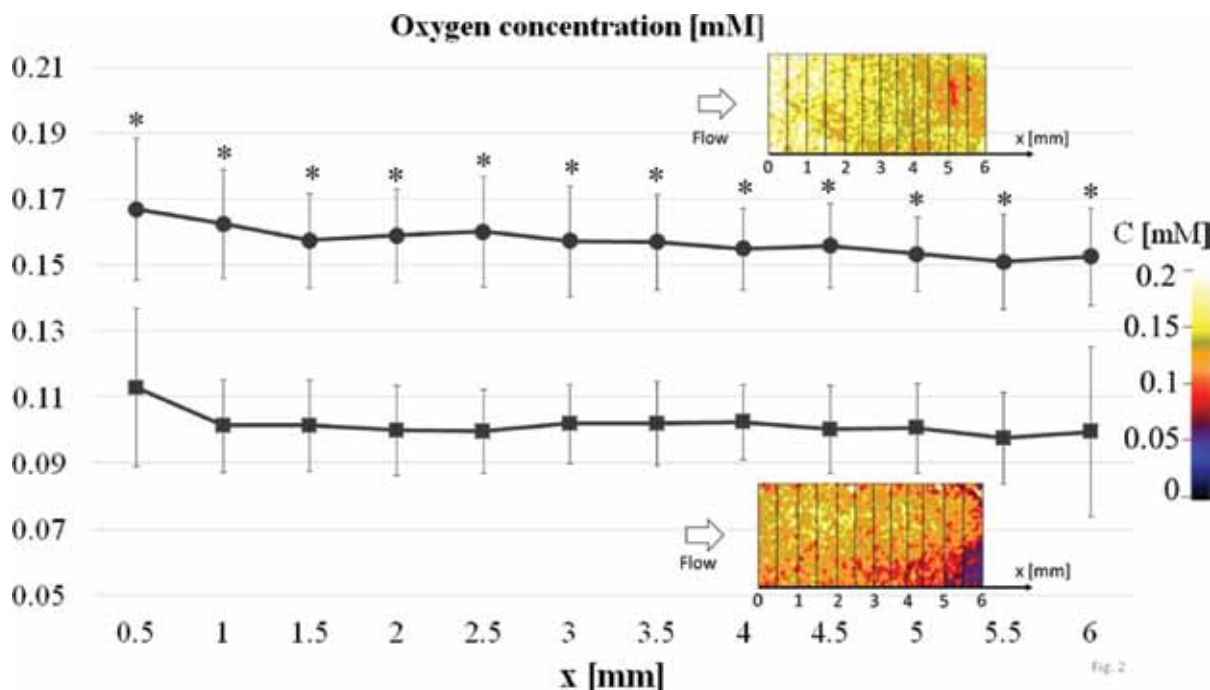


**Fig. 2** - Average oxygen concentration of the three experiments throughout the scaffold regions. The two curves refer to the global maximum (●) and minimum (■) concentration times registered at day 0 and at 1.5 days, respectively. The two line graphs have a similar globally decreasing profile and differ from each other of about 0.057 mM. The curve at day 0 decreases from a mean oxygen concentration in the inlet region of 0.167 to 0.152 mM in the outlet region, while the curve at day 1.5 covers a range of values from 0.113 to 0.995 mM.

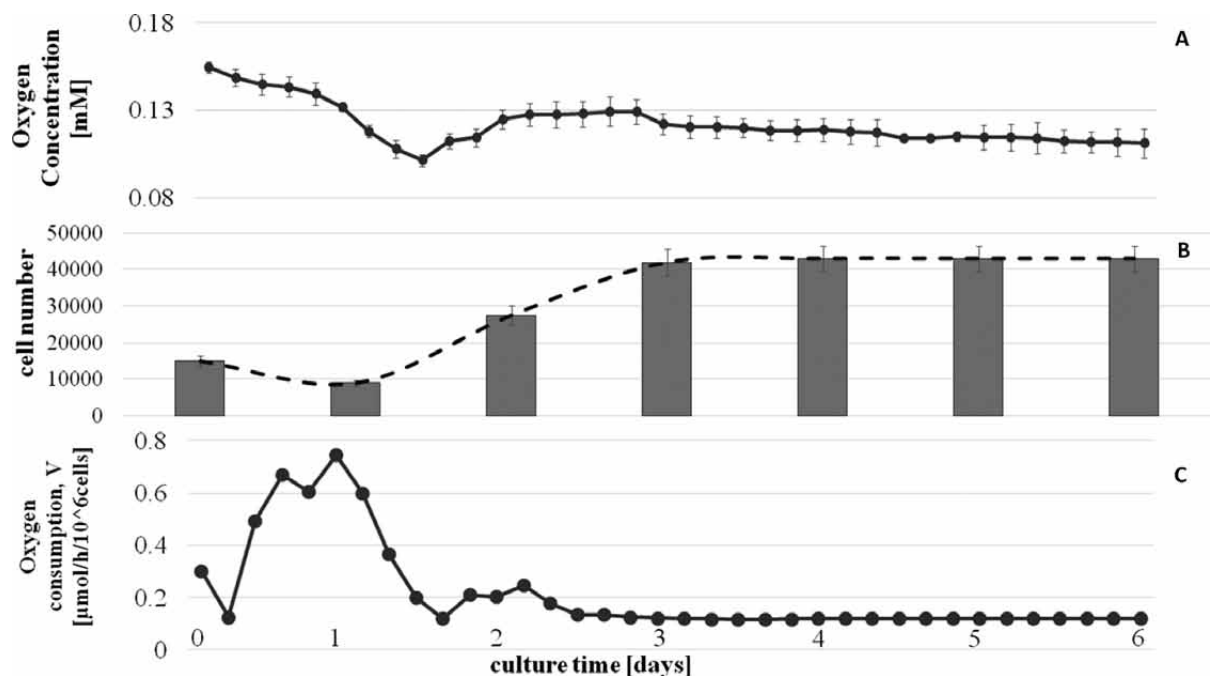


**Fig. 3** - (A) Temporal evolution of oxygen concentration of the whole scaffold. During the first six culture days, oxygen maps were acquired every four hours. The mean oxygen concentration variation shows a globally decreasing profile, which begins with the maximum value of 0.155 mM and drops significantly at around 1.5 days, reaching the minimum value of 0.101 mM. The concentration then recovered a little and ended with a fairly steady segment at a value of 0.113 mM. (B) Results of fluorescence counting. During the first day the cell number in the scaffold decreased from 15 to 8 thousands. A predominant cell expansion (from 8 to 42 thousands of cells) was observed in the period from 1 to 3 days of perfusion then ceased after the fourth culture day. (C) Average oxygen consumption over a 6-days culture time. The curve shows values ranging from approximately a minimum of 0.1 to a peak of 0.7  $\mu\text{mol/h}/10^6\text{cells}$  registered at the first culture day. The oxygen consumption then decreases, stabilizing at its minimum value after about 2.5 days.



seem to be poorer in oxygen than the central part, coherently with the parabolic profile of the culture medium flow. The two line graphs have a similar globally decreasing profile and differ from each other by about 0.057 mM (35% decrease), as demonstrated by darker colours at minimum concentration time oxygen map. The curve at day 0 decreases from a mean oxygen concentration of 0.167 mM in the inlet region to 0.152 mM in the outlet region (9% drop), while the curve at day 1.5 covers a range of values from 0.113 to 0.995 mM (12% drop).

The temporal evolution of oxygen concentration of the whole scaffold over the first six culture days is resumed in Figure 3A. The data representing this graph have been obtained by evaluating the oxygen maps acquired every four hours for six days, on a total 36 time points. The mean oxygen concentration shows a globally decreasing profile which begins with a value of 0.155 mM, to end at 0.113 mM after six days of culture (28% total drop). Oxygen concentration dropped significantly at around 1.5 days reaching a minimum value of 0.101 mM, then slightly recovered and decreased to a constant value. It was possible to estimate the cell proliferation through fluorescence microscopy, in a non-destructive way, during culture time. The results of fluorescence counting are shown in Figure 3B. During the first day, a reduction of cells in the scaffold occurred (from 15 to 8 thousand of cells). Conversely, cell expansion was evident (from 8 to 42 thousand of cells) in the period from 1 to 3 days of perfusion, then ceased after the fourth culture day and the cell number remained constant. Given a certain cell density per scaffold and the previously determined oxygen consumption, we were able to calculate the average oxygen consumption of cells through equation (2). The results over a 6-day culture time are illustrated in Figure 3C and show values ranging from approximately 0.1 to 0.7  $\mu\text{mol}/\text{h}/10^6$  cells. The oxygen consumption reaches a peak at the first culture day and then decreases, stabilizing after about 2.5 days at its minimum value.

Taken all together, the graphs of Figure 3 can be interpreted as follows. The decrease of cell number in the first culture day is probably due to the detachment of weakly adhered cells caused by the hydrodynamic shear stress. During this period, the cell-specific oxygen consumption registers a peak; because of their reduced numbers, cells consume higher quantities of oxygen, largely available in the initial times of culture. Consequently, the oxygen concentration of the whole scaffold drops. Between day 1 and day 3, a massive cell proliferation occurs and the number of cells increases by 425%, while the oxygen consumption quickly decreases due to the reduction of the local oxygen availability. In the last culture days (from day 3 to day 6) cell expansion arrests due to space restrictions, thus both oxygen concentration and consumption stabilize.

## Discussion

Nutrient and oxygen supply to cells are crucial requirements in tissue engineering. If a sufficient supply cannot be guaranteed, the development of the tissue will slow down or be impaired. For example, an oxygen concentration decrease of 84% was predicted by a computational model

within the depth of myocyte-seeded cellularized constructs maintained in static culture (10), while a  $\text{pO}_2$  drop of 95% was found in chondrocytes-seeded constructs that were cultured suspended in spinner flasks, and measured for  $\text{pO}_2$  drops at several time points, after their transfer in a static culture chamber equipped with the oxygen sensor for the measurements (8). Others measured a drop of around 21% in oxygen tension, in a model of cellularized construct perfused by a single capillary-like channel, only assessed in the construct region at the greatest distance from the capillary (11). However, in all the above-cited previous works, the oxygen drops were either predicted theoretically, or measured at fixed time points in static conditions, or measured only in areas very far from the construct area perfused with the culture medium. In this work, for the first time the oxygen drops and cell densities were measured on live constructs non-destructively, without suspending the construct perfusion, through an optically accessible measuring window equipped with an oxygen sensor foil. By this method, we could estimate the spatio-temporal evolution of oxygen concentration, cell density and cell-specific oxygen consumption in 3D cellularized constructs maintained under interstitial perfusion. This condition is known to improve oxygen delivery by forcing its penetration into the scaffold bulk, greatly reducing the oxygen drop in cellularized constructs, while improving the outlet oxygen pressure by up to 34% with respect to surface-perfused constructs, as simulated in a microfluidic setting (12).

In our experiments, cells were uniformly distributed throughout the scaffold at the beginning of culture. Oxygen concentration was higher in the regions of the constructs near the inlet of the culture medium and progressively decreased in the regions near the outlet. We measured an average drop of 10.5% in oxygen concentration between the inlet and outlet of the perfused construct. This value was compared with those reported by the only previous experimental study on interstitial perfusion (4). In their work they measured an oxygen drop of 55%, noticeably higher than our value. The reasons for this discrepancy are: the different type of cells seeded (chondrocytes), which have a lower metabolic rate, their higher density (13 million cells vs. 15 thousand cells) and the different flow rate of culture medium.

The influence of oxygenation on tissue growth was investigated in several numerical studies (4, 13, 14). In a model comprising the whole cellularized construct, the predicted inlet-outlet drop within a 3 mm-thick scaffold was reduced by 11%, coherently with our measurements (12). Most computational models focus on a cuboid region of interest (ROI) of the construct, whose dimensions are considerably smaller than the whole scaffold. For this reason, the calculated drops between the inlet and the outlet cannot be directly compared with our measurements that refer to the whole scaffold. The predicted oxygen drop was found to be comparable in several of these studies: 14% (3), 5% (13) and 2.5% (14). If extended to real scaffold dimensions, the latter two predictions are consistent with our measured data.

Concerning the temporal evolution of oxygen concentration of the whole scaffold, its monitoring may be aimed at

verifying that the minimum  $O_2$  concentration value is maintained above the critical threshold value of hypoxia, believed to be in the order of 2% (15). In our experiments, the tension dropped by 34% between day 1 and day 2 of culture, corresponding to the proliferation phase, and by 28% in the overall culture period, and the minimum tension never fell below 10% in partial pressure. Others report results in general agreement with these general figures. Liu seeded transgenic cells onto porous ceramic particles, incubating them in flow perfusion bioreactors for four days (16). Their results show a global decreasing oxygen profile, with a drop of about 31% between the first and the last culture day, similar to our measured total drop of 28%.

The method adopted for the cell number estimation was based on live imaging (9). This method has proven to be very reliable in distinguishing cell detachment from cell death in live constructs, because it is based on the visual count of labelled cell nuclei, instead of being based on the chemical conversion of a colored dye, like the Alamer blue test for example. Qualitatively, in our experiments cells are partially washed away in the first culture day then cell proliferation shows a first stage of exponential growth, followed by a slowdown when the void volume fraction is reduced. A similar tendency was predicted both computationally (17), as well as measured experimentally (10). While the measurement of oxygen concentration in cellularized constructs has been extensively investigated in several studies, considerably less attention has been paid to quantification of the cell-specific oxygen consumption rate. This parameter widely depends on the type of cells seeded and on their density within the scaffold. The range of values we calculated for immortalized cells goes from 0.1 to 0.7  $\mu\text{mol}/\text{h}/10^6$  cells, which is one order of magnitude higher than the values specific for chondrocytes (18). The peak registered in the first culture day indicates that cells have higher metabolic demands when their number is low, in accordance with Liu's experiment where, after 1 day, cells great viability caused an  $O_2$  deficiency (16).

Our results can be directly compared to the computational predictions obtained in a model of tissue growth referred to the mini-bioreactor system used here (19). The computed oxygen drop on the construct surface between the inlet and outlet regions of the construct was 8%, in good agreement with our measurements. However, at initial conditions, the local oxygen levels predicted by the model were greater by 0.045 mM in all the construct regions, because an inlet oxygen concentration of 0.2 mM, corresponding to saturation, was assumed in the model. Our measurements allowed us to estimate a lower inlet tension for the culture medium, equal to 0.155 mM, in contrast with the value assumed in the model, indicating that the culture medium is not oxygen-saturated when entering the bioreactor. Also, the model assumed a constant oxygen cell consumption rate, instead of the varying rates measured here.

According to the reported results, we can identify limitations of our measurements. Firstly, we measured oxygen consumption for an immortalized cell line and not for other cell types. Immortalized cells are known to be very active metabolically, thus our finding represents the worst possible case in the range of oxygen drops measurable in our perfusion system,

and will be useful for the design of experiments with other cell types using our mini-bioreactor system, as well. Also, we monitored oxygen only on the surface in contact with the sensor foil. In this regard, future developments may be oriented towards attempts to investigate the oxygen concentration also in the deepest regions of the cellularized construct. A further step ahead will consist of imposing different values of the culture medium flow rate, which we set to a constant value in our experiments. A dynamic variation of this parameter will help to minimize the initial cellular detachment phenomenon and optimize cell proliferation and tissue growth.

### Acknowledgement

The authors are very grateful to Matteo Laganà, Domenico Biondi, Pierfrancesco Capone, Tommaso Cazzato, and Samuele Colombo for their expert help.

### Disclosures

Financial support: This project has received partial funding from the European Research Council (ERC) under the European Union's Horizon 2020 research and innovation programme (grant agreement No. 646990 - NICHOID). These results reflect only the authors' view and the Agency is not responsible for any use that may be made of the information contained.

Conflict of interest: The authors have nothing to disclose.

### References

1. Kasper C, van Griensven MR. Bioreactor Systems for Tissue Engineering. 2008, Vol. 112.
2. Liu Y, Wang S. 3D inverted opal hydrogel scaffolds with oxygen sensing capability. *Colloids Surf B Biointerfaces*. 2007;58(1):8-13.
3. Martin Y, Vermette P. Bioreactors for tissue mass culture: design, characterization, and recent advances. *Biomaterials*. 2005; 26(35):7481-7503.
4. Cioffi M, Küffer J, Ströbel S, Dubini G, Martin I, Wendt D. Computational evaluation of oxygen and shear stress distributions in 3D perfusion culture systems: macro-scale and micro-structured models. *J Biomech*. 2008;41(14):2918-2925.
5. Wang L, Acosta MA, Leach JB, Carrier RL. Spatially monitoring oxygen level in 3D microfabricated cell culture systems using optical oxygen sensing beads. *Lab Chip*. 2013;13(8):1586-1592.
6. Grist SM, Chrostowski L, Cheung KC. Optical oxygen sensors for applications in microfluidic cell culture. *Sensors (Basel)*. 2010;10(10):9286-9316.
7. Acosta MA, Ymele-Leki P, Kostov YV, Leach JB. Fluorescent microparticles for sensing cell microenvironment oxygen levels within 3D scaffolds. *Biomaterials*. 2009;30(17):3068-3074.
8. Kellner K, Liebsch G, Klimant I, et al. Determination of oxygen gradients in engineered tissue using a fluorescent sensor. *Bio-technol Bioeng*. 2002;80(1):73-83.
9. Laganà M, Raimondi MT. A miniaturized, optically accessible bioreactor for systematic 3D tissue engineering research. *Biomed Microdevices*. 2012;14(1):225-234.
10. Radisic M, Marsano A, Maidhof R, Wang Y, Vunjak-Novakovic G. Cardiac tissue engineering using perfusion bioreactor systems. *Nat Protoc*. 2008;3(4):719-738.
11. Lovett M, Rockwood D, Baryshyan A, Kaplan DL. Simple modular bioreactors for tissue engineering: a system for characterization of oxygen gradients, human mesenchymal stem cell



- differentiation, and prevascularization. *Tissue Eng Part C Methods*. 2010;16(6):1565-1573.
12. Cantini M, Fiore GB, Redaelli A, Soncini M. Numerical fluid-dynamic optimization of microchannel-provided porous scaffolds for the co-culture of adherent and non-adherent cells. *Tissue Eng Part A*. 2009;15(3):615-623.
  13. Shipley RJ, Jones GW, Dyson RJ, et al. Design criteria for a printed tissue engineering construct: a mathematical homogenization approach. *J Theor Biol*. 2009;259(3):489-502.
  14. Sacco R, Causin P, Zunino P, Raimondi MT. A multiphysics/multiscale 2D numerical simulation of scaffold-based cartilage regeneration under interstitial perfusion in a bioreactor. *Biomech Model Mechanobiol*. 2011;10(4):577-589.
  15. Consolo F, Fiore GB, Truscello S, et al. A computational model for the optimization of transport phenomena in a rotating hollow-fiber bioreactor for artificial liver. *Tissue Eng Part C Methods*. 2009;15(1):41-55.
  16. Liu J, Barradas A, Fernandes H, et al. In vitro and in vivo bioluminescent imaging of hypoxia in tissue-engineered grafts. *Tissue Eng Part C Methods*. 2010;16(3):479-485.
  17. Galbusera F, Cioffi M, Raimondi MT. An in silico bioreactor for simulating laboratory experiments in tissue engineering. *Biomed Microdevices*. 2008;10(4):547-554.
  18. Zhou S, Cui Z, Urban JP. Nutrient gradients in engineered cartilage: metabolic kinetics measurement and mass transfer modeling. *Biotechnol Bioeng*. 2008;101(2):408-421.
  19. Nava MM, Raimondi MT, Pietrabissa R. A multiphysics 3D model of tissue growth under interstitial perfusion in a tissue-engineering bioreactor. *Biomech Model Mechanobiol*. 2013;12(6):1169-1179.